



Universiteit
Leiden
The Netherlands

Chemical biology of glucosylceramide metabolism fundamental studies and applications for Gaucher disease

Oussoren, S.V.; Oussoren S.V.

Citation

Oussoren, S. V. (2017, September 28). *Chemical biology of glucosylceramide metabolism fundamental studies and applications for Gaucher disease*. Retrieved from <https://hdl.handle.net/1887/55842>

Version: Not Applicable (or Unknown)

License: [Licence agreement concerning inclusion of doctoral thesis in the Institutional Repository of the University of Leiden](#)

Downloaded from: <https://hdl.handle.net/1887/55842>

Note: To cite this publication please use the final published version (if applicable).

Cover Page



Universiteit Leiden



The handle <http://hdl.handle.net/1887/55842> holds various files of this Leiden University dissertation

Author: Oussoren, Saskia

Title: Chemical biology of glucosylceramide metabolism : fundamental studies and applications for Gaucher disease

Date: 2017-09-28

Intralysosomal stabilization of
glucocerebrosidase by LIMP-2:
potential implications for efficacy of ERT

Intralysosomal stabilization of glucocerebrosidase by LIMP-2: potential implications for efficacy of ERT

Based on

Paulo Gaspar¹, Saskia Oussoren², Saskia Scheij¹, Marri Verhoek², Rolf Boot²,
Hermen S. Overkleeft³, Jan Aten⁴, Johannes M. Aerts²

¹Dept. Med. Biochem, AMC, Amsterdam

²Dept. Med. Biochem., Leiden University

³Dept. Bio.Synthesis, Leiden University

⁴Dept. Pathology, AMC, Amsterdam

Manuscript in preparation

Abstract

Deficiency of the lysosomal enzyme glucocerebrosidase (GBA) occurs in patients with Gaucher disease (GD) as well as individuals with Action Myoclonus Renal Failure (AMRF). GD is caused by mutations in the *Gba* gene encoding GBA, whilst AMRF is due to mutations in the *SCARB2* gene encoding the lysosomal membrane protein LIMP-2 that governs transport of newly formed GBA to lysosomes. AMRF manifests primarily as a neurological disorder without major visceral complications except for late onset renal disease. In contrast, the common non-neuronopathic (type 1) manifestation of GD is caused by visceral complications due to accumulation of macrophages laden with glucosylceramide, the major GBA substrate. For type 1 GD macrophage-targeted enzyme replacement therapy (ERT) is a registered treatment. For AMRF no treatment is presently available. Since deficiency of GBA is the prominent biochemical abnormality in AMRF patients, we studied the feasibility to supplement LIMP-2 deficient cells with recombinant enzyme. Studies were conducted with normal and AMRF fibroblasts as well as normal and LIMP-2 deficient HEK293 cells transduced with mannose receptor to promote uptake of mannose-terminated recombinant GBA. In LIMP-2 deficient cells, the endocytosed enzyme is abnormally fast proteolytically degraded in lysosomes. The half-life of the GBA in LIMP-2 deficient lysosomes is much shorter than in corresponding normal organelles. This suggests that inside the lysosome transient interactions of GBA with LIMP-2 stabilize the conformation of the enzyme and thus slow down proteolytic breakdown. Such mechanism implies that the efficacy with which lysosomes can be supplemented with GBA is intrinsically capped by LIMP-2 presence. In conclusion, the membrane protein LIMP-2 seems to fulfil a dual purpose in the life cycle of GBA, as transporter and as intralysosomal chaperone.

Introduction

GD is an autosomal recessive disorder caused by impaired glucosylceramide (GlcCer) catabolism as the result of GBA deficiency. The defect leads to prominent storage of GlcCer in lysosomes of macrophages that transform to “Gaucher cells” (lipid-laden macrophages), the hallmark of the disease¹. GBA is encoded by the *GBA* gene and more than 200 different mutations have been described in GD patients^{2,3}. The symptomatology of GD is remarkably heterogeneous, ranging from severe neonatal forms to an almost asymptomatic course. Based on the occurrence and age of onset of the neurological involvement, GD has been classified into acute and juvenile neuropathic forms (types 2 and 3) and the non-neuronopathic forms (type 1)^{1,4,5}. Although there are no strict genotype-phenotype correlations, some mutations are associated with type 1 GD, like the homo- or heteroallelic presence of *GBA* with the N370S mutation. On the other hand, homozygosity for the *GBA* allele with the L444P mutation is associated with a neuropathic form of the disease^{1,6}. Characteristic visceral symptoms of all types of GD are cytopenia, hepatosplenomegaly and skeletal abnormalities^{7,8}.

It was unknown for a long time how GBA reaches the lysosome. In contrast to other lysosomal enzymes, GBA does not acquire phosphomannosyl moieties in its 4 N-linked glycans⁹. The enzyme is targeted to lysosomes by a mechanism independent of the mannose-6-phosphate receptor^{10,11}. Only in 2007, lysosomal integral membrane protein, type 2 (LIMP-2) was identified as the protein responsible for the intracellular sorting of GBA: its absence causes GBA deficiency in almost all organs¹². Mutations in the *SCARB2* gene, encoding the LIMP-2 protein, are the cause of a disorder called Action Myoclonus Renal Failure (AMRF). This disease is characterized by reduced levels of GBA in the majority of cells. Patients develop heterogeneous symptoms such as glomerulosclerosis, progressive myoclonus epilepsy, and ataxia¹³⁻¹⁶. In addition, accumulation of undefined storage material in the brain has been reported¹⁷. Although LIMP-2 deficient individuals share a GBA deficiency with GD patients, AMRF presents markedly different from GD. Most striking is the absence of “Gaucher cells” in AMRF patients and the corresponding lack of elevated plasma chitotriosidase and CCL18¹⁸. Additionally, AMRF patients do not show visceromegaly¹⁶.

Mutations in the *GBA* gene have recently also been linked to Parkinson disease (PD) and Lewy-Body dementia¹⁹⁻²¹. Such increased risk has also been reported for mutations in the *SCARB2* gene²²⁻²⁴. In mice treated with the GBA inhibitor conduritol β -epoxide (CBE), the reduction in GBA activity induces the storage of α -synuclein^{25,26}. Consistently, adenoviral overexpression of GBA in the brain decreases α -synuclein in transgenic mouse models of GD and PD²⁷. Recently, α -synuclein storage was also described in *LIMP-2 KO* mice²⁸.

Already in 1991 enzyme replacement therapy (ERT) for type 1 GD was applied using alglucerase (Ceredase[®]) isolated from human placenta²⁹. This was replaced in 1994 by imiglucerase (Cerezyme[®]) (hrGBA), a recombinant enzyme produced in Chinese hamster ovary cells³⁰. Alternative recombinant enzyme preparations became subsequently available: velaglucerase alfa (VPRIV[®]) produced in a human fibroblast cell line³¹ and Taliglucerase alfa (Elelyso[®]), produced in carrots^{32,33}. All therapeutic GBAs expose terminal mannose residues in order to be efficiently captured by the mannose receptor expressed by macrophages, the

most prominently affected cells in type 1 GD patients²⁹. All ERT treatments are effective for the majority of type 1 GD patients, but the inability of the therapeutic enzymes to cross the blood-brain-barrier prohibits correction or prevention of neuropathology in type 2 and type 3 GD patients. An entirely different approach to treat GD is substrate reduction therapy (SRT). This aims to reduce the levels of GlcCer by inhibiting the biosynthetic enzyme GlcCer synthase (GCS)^{34–38}. Another approach for treating GD is the use of pharmacological chaperones. These compounds are able to promote folding of mutant GBA, promoting its delivery to lysosomes. Inside the lysosome, the chaperone and GBA ideally dissociate and thus the enzyme becomes available to degrade the substrate^{39,40}. Presently, there is no therapy available for AMRF. Although GD and AMRF differ in phenotype, they both share the deficiency in GBA activity. It is therefore of interest to investigate the potential beneficial impact of treating AMRF with approaches similar to the ones successfully employed for GD. Here, we report the outcome of supplementing AMRF cell lines with Cerezyme® (hrGBA). Our investigation has revealed a stabilizing role for GBA of LIMP-2 inside lysosomes. The potential consequences of this interaction are discussed.

Results

LIMP-2 and lysosomal proteolysis of GBA.

To evaluate lysosomal proteolytic degradation, fibroblasts (wild type and AMRF (W178X/W178X SCARB2)) were treated during 4 days with leupeptin, a cysteine and serine protease inhibitor, known to inhibit intralysosomal turnover of GBA⁴¹ (fig. 1). As expected, the presence of leupeptin resulted in increased cellular GBA activity, as detected by enzymatic assay (fig. 1, left panel) and by ABP labelling of active GBA molecules (fig. 1, right panel), both in wild type and AMRF fibroblasts.

The same fibroblast cell lines were supplemented with recombinant GBA (hrGBA) in the medium for 4 days, in the presence or absence of leupeptin (fig. 2). Addition of hrGBA to the medium led to an increase in cellular GBA in the case of control fibroblasts. In contrast, in AMRF fibroblasts almost no increase was observed. The same experiment was conducted in the presence of leupeptin. In all cell lines GBA increased more prominently as measured by enzymatic activity and ABP labeling (fig. 2, left and right panel). Of note, the positive effect of leupeptin was more striking in the case of the AMRF fibroblasts, suggesting that endocytosed GBA is particularly sensitive to lysosomal degradation in these cells.

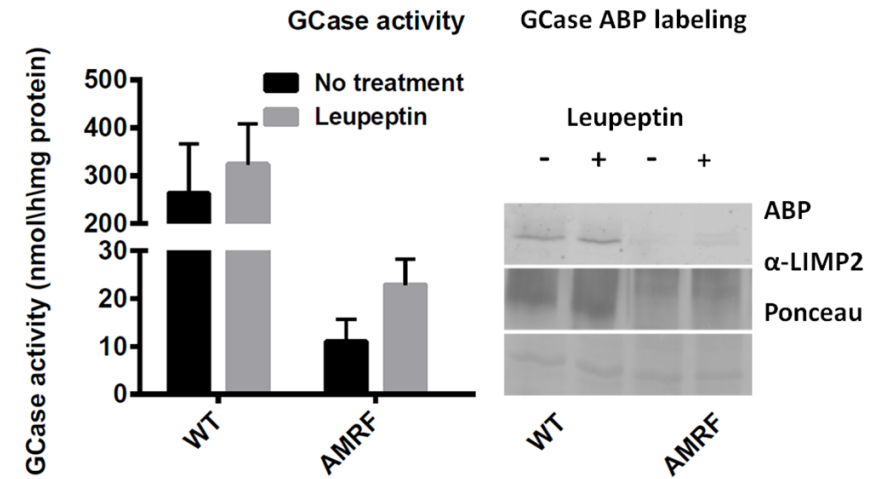


Figure 1. Effect of leupeptin on cellular GBA. Left panel: enzymatic activity of GBA was determined with 4MU-β-Glc; Right panel: ABP labelling followed by SDS-PAGE and fluorescence scanning and detection of LIMP-2 by Western blot. Symbols: – = no treatment; + = Leupeptin 20 μM; WT= wild type; AMRF = LIMP-2 deficient cell line; GD = Gaucher cell line; ABP = activity based probe; GCase = GBA.

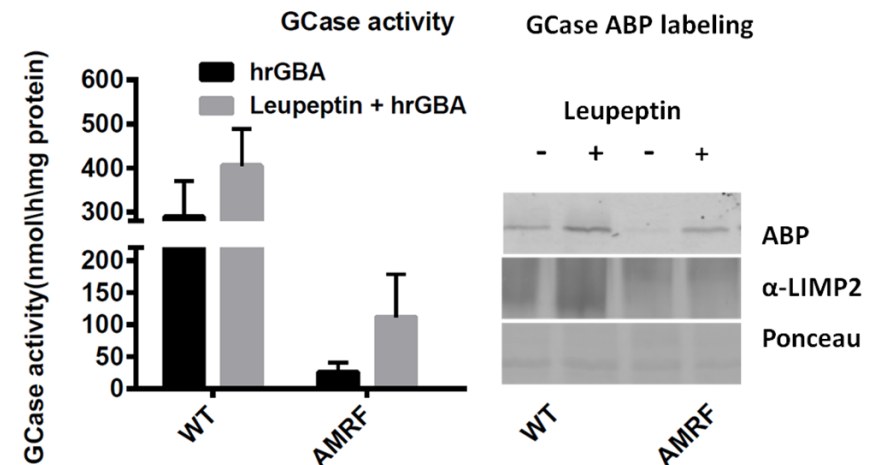


Figure 2. Supplementation of fibroblasts with hrGBA, cultured with or without leupeptin. Left panel: enzymatic activity of GBA was measured with 4MU-β-Glc substrate; Right panel: ABP labelling followed by SDS-PAGE and fluorescence scanning. Detection of LIMP-2 by Western blot. Symbols: – = hrGBA; + = 20 μM Leupeptin plus hrGBA; WT = wild type; AMRF = LIMP-2 deficient cell line; ABP = activity based probe for GBA; GCase = GBA.

Cellular localization of endocytosed hrGBA.

To assess whether hrGBA indeed reaches the lysosome in the case of LIMP-2 deficiency, immunofluorescence experiments were carried out with wild type and AMRF fibroblasts. For this purpose, we combined detection of GBA by ABP labelling with immunohistochemical detection of lysosome using as markers LAMP-2 and LIMP-2 (fig. 3).

Wild type fibroblasts were pre-treated or not with leupeptin and cultured in the presence or absence of hrGBA. In all conditions tested, GBA co-localized with the lysosome marker (LAMP-2) and the amount of active GBA was increased (fig. 3, left panel). In untreated AMRF fibroblasts GBA was barely detectable. In the case of cells treated with leupeptin, some lysosomal GBA in lysosomes became apparent. The amount of GBA was clearly higher in cells that had been exposed to hrGBA (fig. 3, right panel). However, when hrGBA was added to cells in the absence of leupeptin, almost no increase of lysosomal GBA was observed (fig. 3, right panel). These findings suggest that GBA, either endogenous or exogenously added, is particularly sensitive to lysosomal degradation in AMRF fibroblasts.

Role of LIMP-2 in stability of hrGBA as assessed in modified HEK293 cells.

Given the observed marked instability of GBA in lysosomes of AMRF fibroblasts, we attempted to reproduce this finding in cells with an introduced LIMP-2 deficiency. For this, we constructed HEK293 cells deficient in LIMP-2 by knock-out of the *SCARB2* gene using CRISPR technology. In addition, HEK293 cells were stably transfected with cDNA encoding the mannose receptor (MR). MR-positive cells can more efficiently internalize hrGBA with terminal mannose residues in its N-linked glycans. With the different HEK293 cell lines (+/- LIMP2; +/- MR), the same experiments were conducted as with fibroblasts (fig. 4). Wild type HEK293 cells (expressing MR or not) showed a modest increase in cellular GBA in the presence of leupeptin. LIMP-2 deficient HEK293 cells showed a more evidently increased GBA activity in the presence of leupeptin (fig. 4, left panel). Thus, the findings with fibroblasts were recapitulated with the modified HEK293 cells.

The presence of hrGBA in the culture medium led to marked increase in cellular GBA in wild type HEK293 cells, particularly those transfected with MR. Cellular GBA activity was only slightly further increased by leupeptin (fig. 4, right panel). In contrast, in LIMP-2 deficient HEK293 cells the exposure to hrGBA hardly increased GBA activity, even in those cells expressing MR (fig 4, right panel). However, concomitant presence of leupeptin resulted in a very prominent increase of cellular GBA activity. Levels of cellular GBA in the LIMP-2 deficient HEK293 cells were almost identical to those in corresponding wild type cells (fig 4, right panel). Thus, endogenous as well as exogenous GBA in lysosomes of LIMP-2 deficient cells appears to be more susceptible to leupeptin-sensitive proteolytic degradation.

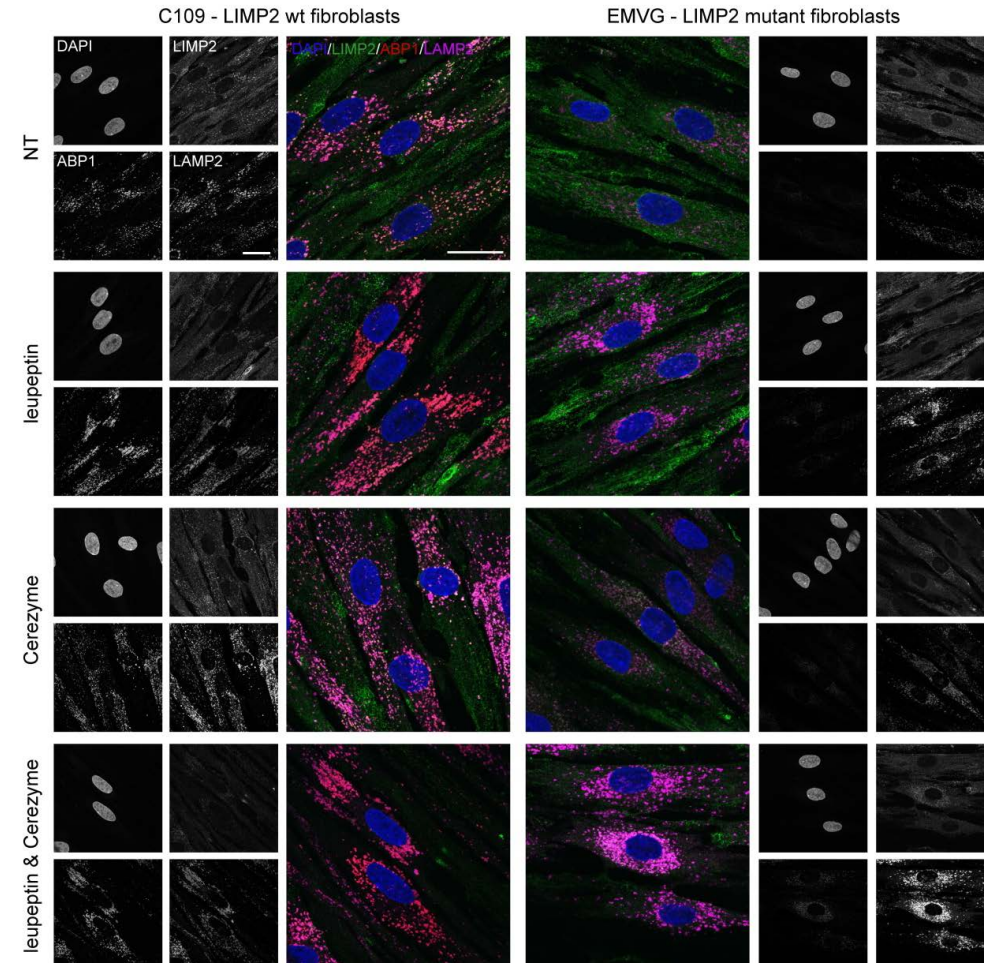


Figure 3. Detection of GBA in wild type and AMRF fibroblasts. Cells were treated with or without leupeptin and with hrGBA. Left panel: wild type fibroblasts; Right panel; AMRF fibroblasts. ABP1 = Activity based probe for GBA; DAPI = Nucleus staining.

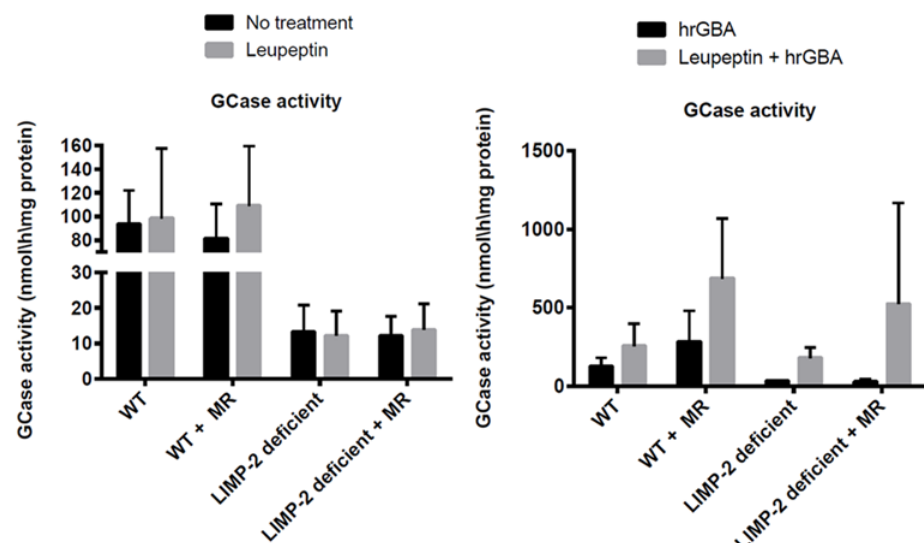


Figure 4. GBA activities in WT and LIMP-2 deficient HEK293 cells with or without MR: effect of LIMP-2 on supplementation by exogenous GBA (hrGBA). Cellular GBA was measured with 4MU- β -Glc substrate. Left panel: Cells not exposed to exogenous hrGBA; Right panel: Cells exposed to exogenous hrGBA. MR = mannose receptor; GCase = GBA.

Comparable uptake of hrGBA by wild type and LIMP-2 deficient HEK293 cells.

To evaluate whether the uptake of hrGBA is normal in LIMP-2 deficient cells, excess hrGBA was added to the various HEK293 cells with or without MR at 10 °C to saturate surface receptors. Next, cells were chased at 37 °C for 15 min in the presence of enzyme, washed and chased further without enzyme for different time periods. Cells were harvested at different time points (triplicate wells) and analyzed on GBA. Leupeptin was present during the entire experiment.

Uptake of hrGBA was very similar in wild type and LIMP-2 deficient HEK293 cells without MR for the first 15 min (Table 1). Uptake was equally higher in wild type and LIMP-2 deficient HEK293 cells expressing MR (Table 1).

Lack of overt change in lysosomal proteases in LIMP-2 deficient cells.

We determined the proteome of isolated lysosomes from hepatocytes of wild type and LIMP-2 KO mice. Careful inspection of soluble lysosomal proteases showed no significant differences, see Table 2.

The intralysosomal breakdown of GBA is prevented by the lysosomal cysteine cathepsin inhibitors E64 and the structurally related activity-based probe DCG-04⁴²⁻⁴⁴. Fluorescently (BODIPY) tagged DCG-04 allows visualization of its target cathepsins. Figure 5 shows no differences in labeled cathepsins in wild type and LIMP-2 deficient HEK293 cells. Thus, GBA

itself seems more prone for degradation in LIMP-2 deficient lysosomes compared to normal organelles.

Table 1. Uptake of hrGBA in HEK293 cells. HEK293 cells (+/- LIMP-2; +/- MR) were pre-loaded 10 °C with saturating hrGBA, chased for 15 minutes at 37 °C, washed and chased further until 1 h without enzyme. Cells were harvested at indicated time points. Cellular GBA was measured with the fluorescent substrate 4MU- β -Glc. The cellular GBA present prior to uptake was subtracted: shown is the increment in cellular GBA activity.

Increment in cellular GBA in HEK293 cells exposed to hrGBA and leupeptin (nmol hydrolysis/ h/ mg protein)				
TIME (MIN)	WT	LIMP2 DEF	WT + MR	LIMP2 DEF +MR
0	18 ± 5	17 ± 6	58 ± 11	54 ± 13
5	22 ± 6	19 ± 7	60 ± 10	55 ± 10
7.5	36 ± 6	34 ± 5	93 ± 9	88 ± 11
10	51 ± 9	48 ± 8	133 ± 22	116 ± 15
12.5	64 ± 18	61 ± 10	150 ± 23	147 ± 18
15	70 ± 12	71 ± 49	180 ± 11	157 ± 12
20	83 ± 19	80 ± 15	232 ± 32	193 ± 13
25	90 ± 13	84 ± 16	259 ± 22	245 ± 19
30	93 ± 24	82 ± 10	230 ± 18	251 ± 11
40	98 ± 15	83 ± 9	240 ± 10	220 ± 9
60	99 ± 13	76 ± 20	262 ± 15	218 ± 20

Stability of hrGBA in wild type and LIMP-2 deficient lysosomes.

Next, fibroblasts from a control subject and AMRF patient (W178X/W178X SCARB2) were incubated with hrGBA for 4 days and then chased for different time points (fig. 6). The reduction in cellular GBA activity during the chase was very prominent in AMRF fibroblasts when compared to wild type and GD cells (fig 6a). The half-life of GBA in the AMRF fibroblasts was only about 6-8 h vs >48 h in the corresponding wild type cells (fig. 6b).

To assess whether the lifetime of hrGBA differs in wild type and LIMP-2 deficient lysosomes, a 9 h chase of endocytosed hrGBA was performed in wild type and AMRF fibroblasts in the presence of leupeptin (fig. 7). In the presence of the protease inhibitor the stability of GBA following uptake was very similar in various fibroblasts as determined by enzymatic assay and ABP labeling. This observation, combined with the findings in the absence of leupeptin (fig. 6), indicates that leupeptin-sensitive proteolytic turnover of exogenous hrGBA occurs faster in AMRF lysosomes than in wild type lysosomes.

Table 2. Lysosomal matrix proteases in tritosomes obtained from wild type and LIMP-2 deficient mouse livers.

PROTEIN NAME	ACCES Nº	DESCRIPTION	RATIO
CATH_MOUSE	P49935	Pro cathepsin H OS Mus musculus GN Ctsh PE 2 SV 2	1.22
CATL1_MOUSE	P06797	Cathepsin L1 OS Mus musculus GN Ctsl1 PE 1 SV 2	0.98
CATZ_MOUSE	Q9WUU7	Cathepsin Z OS Mus musculus GN Ctsz PE 2 SV 1	1.12
DPP2_MOUSE	Q9ET22	Dipeptidyl peptidase 2 OS Mus musculus GN Dpp7 PE 2 SV 2	0.87
LGMN_MOUSE	O89017	Legumain OS Mus musculus GN Lgmn PE 1 SV 1	0.96
RISC_MOUSE	Q920A5	Retinoid inducible serine carboxypeptidase OS Mus musculus GN Scep1 PE 2 SV 2	1.12
PCP_MOUSE	Q7TMR0	Lysosomal Pro X carboxypeptidase OS Mus musculus GN Prcp PE 2 SV 2	0.64
CATF_MOUSE	Q9R013	Cathepsin F OS Mus musculus GN Ctsf PE 2 SV 1	0.62
CATS_MOUSE	O70370	Cathepsin S OS Mus musculus GN Ctss PE 2 SV 2	0.78
NICA_MOUSE	P57716	Nicastrin OS Mus musculus GN Ncstn PE 1 SV 3	1.15
CATB_MOUSE	P10605	Cathepsin B OS Mus musculus GN Ctsb PE 1 SV 2	0.98
TPP1_MOUSE	O89023	Tripeptidyl peptidase 1 OS Mus musculus GN Tpp1 PE 1 SV 2	1.22
PPGB_MOUSE	P16675	Lysosomal protective protein OS Mus musculus GN Ctsp PE 1 SV 1	1.40
CATD_MOUSE	P18242	Cathepsin D OS Mus musculus GN Cttd PE 1 SV 1	n.d.

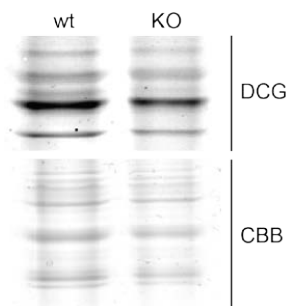


Figure 5. Labeling of cathepsins in wild type and LIMP-2 deficient HEK293 cells with BODIPY DCG-04. HEK293 cells were incubated for 60 minutes with BODIPY DCG-04 and labeled cathepsins were visualized by fluorescence scanning after SDS-PAGE (upper panel); Total cellular protein as visualized by staining with CBB (lower panel).

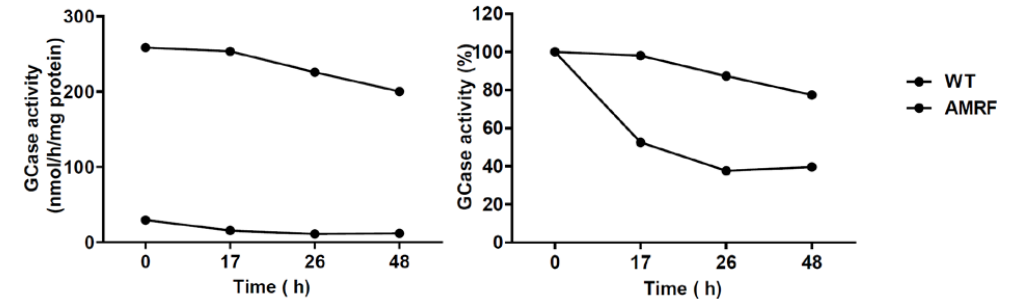


Figure 6. Chase of endocytosed hrGBA in different fibroblast cell lines. Fibroblasts were incubated with hrGBA for 4 days. Cells were harvested and GBA activities were measured with the fluorescent substrate 4MU-β-Glc. Left panel: absolute GBA activity; Right panel: Half-life of GBA. Upper lines: WT fibroblasts; Lower lines: AMRF fibroblasts; GCCase = GBA.

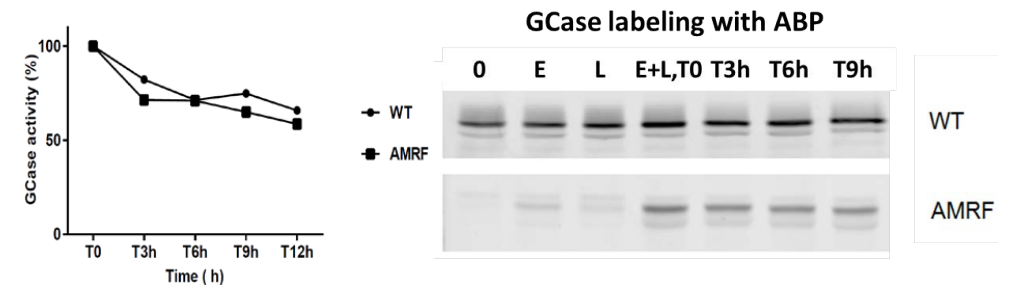


Figure 7. Half-life of hrGBA in the presence (+) of leupeptin. Fibroblasts were incubated with hrGBA (E) in the absence and presence of leupeptin (L), and chased for 9 hours. Cells were harvested and GBA activity was determined in lysates using 4MU-β-Glc substrate. Left panel: activity at T0 is expressed as 100 % for each cell line. Active GBA (GCCase = GBA) was visualized by ABP labeling (right panel).

Lastly, the half-life of exogenous GBA was determined in HEK293 cells expressing MR in the absence of protease inhibitor. Cells were cultured for 3 days with hrGBA, extensively washed and chased in the same medium for different time points. Every two days the medium was refreshed. The cellular GBA content at the start of the chase was lower in LIMP-2 deficient cells (Table 3). It also declined much faster in LIMP-2 deficient HEK cells than the wild type counter parts. The estimated half-life of GBA was 28.3 h in wild type HEK293 cells and only 6.2 h in LIMP-2 deficient cells.

Table 3. Chase of hrGBA in HEK293 cells with MR, following uptake of enzyme for 3 days, in the absence of protease inhibitor: estimated half-life.

	WT +MR	LIMP2 DEF + MR
Cellular GBA After 3 D Pulse With hrGBA (nmol/H/ mg prot)	520 ± 120	36 ± 9
Half-Life GBA During Chase (H)	28.3 ± 3.2	6.2 ± 1.4

Discussion

The key role of LIMP-2 in sorting GBA from the ER to lysosomes has been unequivocally demonstrated. Binding of newly formed GBA to a specific domain in LIMP-2 governs its routing^{12,45,46}. It has been proposed that at low pH the complex LIMP-2/GBA dissociates and enzyme is released⁴⁷. However, binding of GBA to LIMP-2 is not completely abolished at pH values below 6.0. It is therefore conceivable that even inside lysosomes GBA and LIMP-2 may transiently bind, with beneficial effects on the conformation of GBA and subsequent increased resistance of the enzyme against proteolytic breakdown. To study this possibility we exposed wild type and LIMP-2 deficient HEK293 cells to leupeptin, an inhibitor of the lysosomal serine and cysteine proteases. Leupeptin is well known from metabolic labeling experiments using 35C-methionine incorporation to effectively reduce intralysosomal degradation of GBA⁴¹. Indeed we noted an increase in cellular GBA of wild type fibroblasts with enzyme assay and ABP-labeling alike in the presence of leupeptin. In the case of AMRF fibroblasts however, leupeptin lead to a much more pronounced increase in cellular GBA. This suggests that the small amount of GBA that manages to reach lysosomes during LIMP-2 deficiency has to be far more prone to intralysosomal leupeptin-inhibitable proteolytic degradation. This difference between wild type and LIMP-2 fibroblasts became even more apparent when cells were incubated with recombinant GBA (hrGBA). Again, in AMRF cells, the endocytosed hrGBA appeared far more sensitive to proteolytic, leupeptin-inhibitable, degradation as compared to the situation in wild type fibroblasts. The average half-life of endocytosed hrGBA in AMRF fibroblasts in the absence of leupeptin was surprisingly short, being only about 6 - 8 h.

To exclude that the observed differences between wild type and AMRF fibroblasts were due to other genetic differences beyond the *SCARB2* gene, we generated LIMP-2 deficient HEK293 cells by CRISPR technology. Comparison of wild type and LIMP-2 deficient HEK293 cells, equipped or not with mannose receptor, again revealed that exogenous GBA in LIMP-2 deficient lysosomes is far more vulnerable to leupeptin-inhibitable proteolytic breakdown.

We investigated with the same HEK293 cells whether LIMP-2 may be involved in uptake of GBA, a possible mechanism since low amounts of LIMP-2 are supposedly transiently

present at the cell surface. However, no evidence for this was obtained in experiments with wild type and LIMP-2 deficient HEK293 cells, equipped with mannose receptor or not. In these experiments we pre-loaded receptors at the cell surface with hrGBA at 10 °C and chased cells for different time periods at 37 °C. During the first hour of chase, leupeptin-inhibitable degradation of GBA was still very small and a good impression could be obtained about uptake rate. Of note, Malini *et al.* recently also reported that hrGBA cellular uptake is independent of LIMP-2⁴⁶.

Longer chase periods allowed us to determine the half-life of endocytosed exogenous GBA, particularly in HEK293 cells expressing mannose-receptor that endocytosed large amounts of enzyme. In wild type HEK293 cells the half-life was 28.3 h, following saturating pre-loading with hrGBA. In comparable LIMP-2 deficient cells expressing mannose receptor it was just 6.2 h. The presence of leupeptin abolished the difference in stability of GBA in wild type and LIMP-2 deficient cells, extending it far over 48 h. Since there are no experimental indications for a different make-up of acid cysteine and serine proteases in LIMP-2 deficient lysosomes, it is attractive to speculate that transient interactions between LIMP-2 and GBA in lysosomes render protection against proteolytic break down of the enzyme. Indeed, Zunke *et al.* recently described that a LIMP-2 helix 5-derived peptide interacts with GBA in lysosomes in intact cells and activates the enzyme in the process⁴⁸.

Our findings may have important implications. It can be envisioned that the amount of LIMP-2 in lysosomes installs an intrinsic limit for the efficacy of ERT. LIMP-2 might become rate-limiting regarding stabilization of exogenous GBA. When too much enzyme is taken up, lack of interaction with the limited amount of LIMP-2 will promote more rapid proteolytic breakdown. Consistent with this is our observation that increase in cellular GBA in mannose receptor expressing HEK293 cells does not seem limited by binding capacity of surface expressed receptor, but rather by intralysosomal stability of endocytosed GBA which relatively decreases with higher dose. A simplified scheme is shown in figure 8, depicting the hypothesis formulated here.

Thus, effectiveness of GBA-ERT may be maximized by the finite presence of LIMP-2 in lysosomes. ERT at very high doses of hrGBA would theoretically result in far excess of exogenous GBA over endogenous LIMP-2 in lysosomes, and the intralysosomal stability of administered enzyme could consequently be poor. Theoretically, administration of very large amounts of hrGBA to cells may even reduce the stability of endogenous GBA due to competition for LIMP-2 stabilization inside lysosomes. It should be considered that the stabilizing effect of LIMP-2 on intralysosomal GBA is more critical in GD patients who concomitantly are carriers for LIMP-2 deficiency. Indeed, it has been reported that carriership for LIMP-2 deficiency acts as modifier and worsens the clinical course of GD⁴⁹.

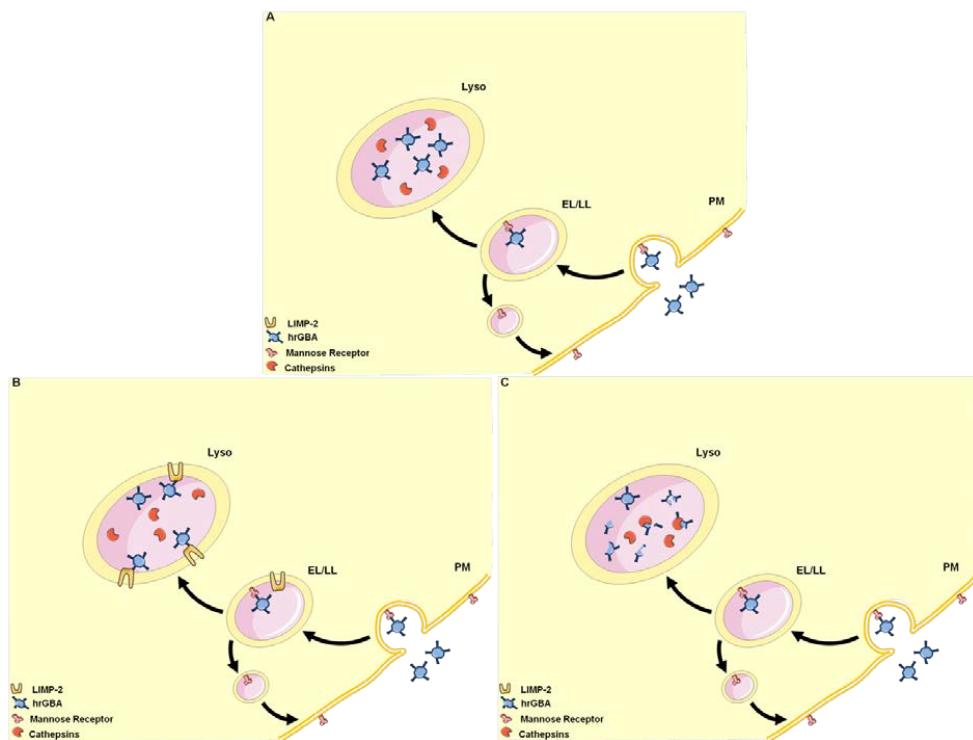


Figure 8. Stability of exogenous hrGBA in wild type and LIMP-2 deficient cells. A. Presently broadly accepted view, ERT for Gaucher Disease; **B.** Proposed model for LIMP-2 as a (lysosomal) chaperone in WT cells; **C.** Proposed model for the detrimental effect of LIMP-2 deficiency in cells, the chaperone lacking in AMRF.

Based on our present concept, ERT of AMRF with recombinant GBA seems not a wise approach. The presently used therapeutic GBAs in ERT of type 1 GD are neither attractive as drug for neurologically affected AMRF patients since these enzymes seem not to pass well the BBB. Other therapeutic approaches such as gene therapy or pharmacological manipulation of the glycosphingolipid metabolism seem to be more attractive to ameliorate abnormalities in AMRF patients. Future studies with LIMP-2 KO mice will be useful to determine which approach is the most appealing to treat AMRF, a disorder with still unmet clinical need.

In conclusion, LIMP-2 seems to influence GBA at various stages of its life cycle. Firstly, LIMP-2 transports newly formed GBA to lysosomes. Secondly, LIMP-2 likely stabilizes GBA also in the lysosome and consequently protects it against proteolytic breakdown. Thus, LIMP-2 seems to have a dual action as transporter and as lysosomal chaperone of GBA.

Materials & Methods

Materials

MDW941 (Inhibitor Red) was synthesized at the Leiden Institute of Chemistry as described earlier^{50,51}. The rabbit polyclonal anti-LIMP-2 antibody was acquired from Novus Biologicals, Littleton, USA (NB400-129). Human recombinant glucocerebrosidase (hrGBA: Cerezyme™) was a gift from Genzyme, Boston, USA. All other chemicals were obtained from Sigma.

Methods

SCARB2 gene knock-out

In human embryonic kidney 293 (HEK293) cells (ATCC CRL 1573) a *SCARB2* gene knock-out was generated using the CRISPR/Cas9 system. Guide RNA sequences were selected using the optimized CRISPR design tool (<http://crispr.mit.edu>) using the individual *SCARB2* exon sequences as template. For the selected guides two complementary oligos containing the *SCARB2* guide sequences and BbsI ligation adapters were annealed and ligated into pX335 (pX335-U6-Chimeric_BB-CBh-hSpCas9n (D10A, Nickase, Addgene plasmid #42335) and digested with BbsI according to the described protocol⁵². Primers used for *SCARB2* exon 1 are: guide 1 5'-CACCGGACGTTGTCCTGCTCCTGC-3' and 5'-AAACGCAGGAGCAGGGACAACGTCC-3'. *SCARB2* exon 1 guide 2 5'-CACCGCCCGCGTGTAGAAGCAGCAT-3' and 5'-AAACATGCTGCTTCTACACGGCGGC-3'. For targeting the *SCARB2* exon 7 primers are: guide 1 5'-CACCGTATACCTGAGGGAACTGCC-3' and 5'-AAACGGCAGTTTCCCTCAGGTATAC-3'. *SCARB2* exon 7 guide 2 5'-CACCGCCGGCATTGTCTGACGTAT-3' and 5'-AAACATACGTACACAATGCCGGCC-3'. HEK293T cells were transfected with a 1:1 ratio of pX335 guide 1 and pX335 guide 2 for either exon 1 or exon 7 of the *SCARB2* gene using FuGene6 (Roche) with a FuGene: DNA ratio of 3:1. Two days after transfection single cell clones were isolated by seeding at 0.5 cell per well in 96 well plates. Clones were checked by PCR and sequencing for the presence of indels. One clone (N1F8) with sequence confirmed indels was shown to secrete GBA. Western blot analysis (data not shown) displayed that clone N1F8 lacks any LIMP-2 protein. HEK293T cells were cultured in DMEM with high glucose, supplemented with 10 % FBS and 100 units/ml Pen/Strep.

Transfection of HEK293 cells with macrophage mannose receptors

HEK293T cells were cultured in DMEM with high glucose (Gibco) supplemented with 10 % FBS (Bodinco) and 100 units/ml Pen/Strep (Gibco). One day before transfection 4×10^5 cells/well were seeded in a 6 well plate. HEK293T cells and HEK293T *SCARB2* knock-out cells (clone N1F8) were infected with a human Mannose Receptor (CD206) pLenti6.3/TO/V5-DEST construct, generated via PCR and the Gateway cloning system (Invitrogen) using primers 5'-GGGGACAAGTTTGTACAAAAAAGCAGGCTTCGGTACCACCATGAGGCTACCCCTGC-3' and 5'-GGGGACCACTTTGTACAAGAAAGCTGGGTCGATGACCGAGTGTTTCATTCTG-3',

and pDONR221 as cloning intermediate. All constructs were verified by sequencing. To produce lentiviral particles, HEK293T cells were transfected with pLenti6.3-CD206 in combination with the envelope and packaging plasmids pMD2G, pRRE and pRSV. Subsequently, culture supernatant containing viral particles was collected and used for infection of HEK293 cells and HEK293 *SCARB2* knockout cells (clone N1F8). Infected cells were selected using blasticidin (Sigma) 2.5 µg/ml.

Cell culture and experiments

Fibroblasts were cultured in DMEM medium supplemented with 10 % fetal bovine serum and 1 % Pen/Strep. HEK293 cells were seeded one day before the experiment at 1×10^6 cells/well in a 6 well plate. The cells were subjected to the following 4 conditions during 4 days: no treatment; 20 µM of leupeptin (a broad spectrum protease inhibitor); 32 ng/µl of human recombinant GBA (hrGBA); and 32 ng/µl of hrGBA for one hour after 20 µM of leupeptin. At the fourth day of exposure, the cells were harvested. To evaluate the effect of leupeptin on hrGBA, cells were exposed to either leupeptin and hrGBA or hrGBA only. At the fourth day, cells were washed with cold PBS, and the cells subsequently cultured with or without leupeptin, as aforementioned.

Uptake of hrGBA

HEK293 cells were seeded one day prior to the experiment at 1×10^6 cells/well in a 6 well plate. The cells were subjected to 32 ng/µl of hrGBA one hour after addition of 20 µM of leupeptin. The following time points were collected: 0, 10, 20, 30 min.

Preparation of cell homogenates

Isolated fibroblasts and HEK293 cells were homogenized by sonication on ice and cellular protein was measured according to the manufacturer's protocol with Pierce™ BCA Protein Assay Kit (Pierce Biotechnology Inc., No. 23225). When necessary lysates were diluted with MilliQ water.

In vitro activity-based probe labeling of GBA, gel electrophoresis and fluorescence scanning

Homogenate (50 µg total protein) was incubated with 100 nM cyclophellitol-epoxide type activity based probe MDW941⁵⁰ in 150 mM Mcllvaine buffer (150 mM citrate- Na_2HPO_4 , pH 5.2. with 0.2 % (w/v) sodium taurocholate, 0.1 % Triton X-100) and protease inhibitor cocktail (Roche) for 45 min at 37 °C. Next, protein was denatured in 5x Laemmli buffer (50 % (v/v) 1 M Tris-HCl, pH 6.8, 50 % (v/v) glycerol, 10 % (w/v) DTT, 10 % (w/v) SDS, 0.01 % (w/v) bromophenol blue) by boiling for 10 min at 100 °C. Proteins were separated by electrophoresis on 10 % (w/v) acrylamide SDS-PAGE gels⁵¹. Wet slab gels were scanned for red fluorescence with a Typhoon variable mode imager (Amersham Bioscience) using λ_{ex} 532 nm and λ_{em} 610 nm (band pass filter 30nm). Fluorescence was quantified using ImageJ software (NIH). Gels were transferred onto a nitrocellulose membrane (Schleicher & Schuell) and protein was visualized with Ponceau S staining⁵¹.

Western blotting

SDS-PAGE gels were electroblotted onto a nitrocellulose membrane (Schleicher&Schuell). Membranes were blocked with 5 % skimmed milk and 0.05 % Tween-20 in Tris-buffered saline (TBS) for 1 h at room temperature and incubated overnight with the primary antibody at 4 °C. Membranes were then washed three times with 0.01 % Tween-20 in TBS and incubated with the appropriate IRDye conjugated secondary antibody for 1 h at room temperature. After washing, detection was performed using the Odyssey® Clx, Infrared Imaging System (LI-COR).

Immunofluorescence analysis

Fibroblasts were cultured on glass slides. The cells were subjected to the following 4 conditions during 4 days: no treatment; 20 µM of leupeptin; 32 ng/µl of hrGBA; 32 ng/µl of hrGBA one hour after of 20 µM of leupeptin. Cells were incubated overnight with 1 nM MDW941 in HAM/DMEM with 10 % FCS. Next, cells were washed, fixed with 3 % (v/v) paraformaldehyde in PBS for 60 min, washed with PBS and incubated with 0.1 % saponin in PBS. They were washed again with PBS, incubated with 0.1 mM NH_4Cl in PBS for 10 min and then with normal antibody diluent (BD09-999; Immunologic, Duiven, The Netherlands) for 2 h. Nuclei were stained with DAPI, LIMP-2 protein with rabbit IgG anti-LIMP-2 antibody (NB400-129, Novus Biologicals, Abingdon, UK) and LAMP-2 protein with mouse IgG1 anti-LAMP-2 antibody (clone H4B4; 9840-01, Southern Biotechnology Associates, Birmingham, AL). Second step antibodies were Alexa Fluor 488-conjugated goat IgG anti-rabbit IgG (A11034; Life Technologies, Bleiswijk, The Netherlands) and ATTO647N-conjugated goat IgG anti-mouse IgG (610-156-121; Rockland, Limerick, PA). Slides were mounted with ProLong Gold (Life Technologies). Imaging was performed by means of confocal laser scanning microscopy using a TCS SP8 X mounted on a DMI 6000 microscope with a Plan APO 63x/1.40 Oil CS2 objective. For excitation were applied a 405 nm UV diode for DAPI, and a 470-670 nm WLL Pulsed laser, sequentially set at 488 nm, 592 nm and 647 nm for the respective fluorochromes. PMT and HyD detection was applied. Recorded images were analyzed and overlaid using LAS X software (Leica Microsystems, Son, The Netherlands).

GBA activity assay

Activity assays were performed as described earlier⁵³. Briefly, GBA activity was measured with 3.73 mM 4-methylumbelliferyl- β -D-glucopyranoside (4MU- β -Glc), dissolved in 150 mM Mcllvaine buffer (pH 5.2 supplemented with 0.2 % (w/v) sodium taurocholate, 0.1 % (v/v) Triton X-100) and 0.1 % BSA. After stopping the reaction with NaOH-glycine (pH 10.3), fluorescence was measured with a fluorimeter LS55 (Perkin-Elmer, Beaconsfield, UK) at λ_{ex} 366 nm and λ_{em} 445 nm.

References

1. E. Beutler, G. A. G. in *C.R. Scriver, W.S. Sly, D. Valle (Eds.), The Metabolic and Molecular Bases of Inherited Disease, 8th ed.* 3635–3668 (McGraw-Hill, New York, 2001).
2. Lee, J.-Y. *et al.* Clinical and genetic characteristics of Gaucher disease according to phenotypic subgroups. *Korean J. Pediatr.* **55**, 48–53 (2012).
3. Hruska, K. S., LaMarca, M. E., Scott, C. R. & Sidransky, E. Gaucher disease: mutation and polymorphism spectrum in the glucocerebrosidase gene (GBA). *Hum. Mutat.* **29**, 567–83 (2008).
4. Baris, H. N., Cohen, I. J. & Mistry, P. K. Gaucher disease: the metabolic defect, pathophysiology, phenotypes and natural history. *Pediatr. Endocrinol. Rev.* **12 Suppl 1**, 72–81 (2014).
5. Mehta, A. Epidemiology and natural history of Gaucher's disease. *Eur. J. Intern. Med.* **17 Suppl**, S2-5 (2006).
6. Ohashi, T. *et al.* Characterization of human glucocerebrosidase from different mutant alleles. *J. Biol. Chem.* **266**, 3661–7 (1991).
7. Boven, L. A. *et al.* Gaucher cells demonstrate a distinct macrophage phenotype and resemble alternatively activated macrophages. *Am. J. Clin. Pathol.* **122**, 359–69 (2004).
8. Bussink, A. P., van Eijk, M., Renkema, G. H., Aerts, J. M. & Boot, R. G. The biology of the Gaucher cell: the cradle of human chitinases. *Int. Rev. Cytol.* **252**, 71–128 (2006).
9. Aerts, J. M. *et al.* Glucocerebrosidase, a lysosomal enzyme that does not undergo oligosaccharide phosphorylation. *Biochim. Biophys. Acta* **964**, 303–8 (1988).
10. Rijnboutt, S., Aerts, H. M., Geuze, H. J., Tager, J. M. & Strous, G. J. Mannose 6-phosphate-independent membrane association of cathepsin D, glucocerebrosidase, and sphingolipid-activating protein in HepG2 cells. *J. Biol. Chem.* **266**, 4862–8 (1991).
11. Rijnboutt, S., Kal, A. J., Geuze, H. J., Aerts, H. & Strous, G. J. Mannose 6-phosphate-independent targeting of cathepsin D to lysosomes in HepG2 cells. *J. Biol. Chem.* **266**, 23586–92 (1991).
12. Reczek, D. *et al.* LIMP-2 Is a Receptor for Lysosomal Mannose-6-Phosphate-Independent Targeting of β -Glucocerebrosidase. *Cell* **131**, 770–783 (2007).
13. Berkovic, S. F. *et al.* Array-Based Gene Discovery with Three Unrelated Subjects Shows SCARB2/LIMP-2 Deficiency Causes Myoclonus Epilepsy and Glomerulosclerosis. *Am. J. Hum. Genet.* **82**, 673–684 (2008).
14. Badhwar, A. *et al.* Action myoclonus-renal failure syndrome: characterization of a unique cerebro-renal disorder. *Brain* **127**, 2173–2182 (2004).
15. Balreira, A. *et al.* A nonsense mutation in the LIMP-2 gene associated with progressive myoclonic epilepsy and nephrotic syndrome. *Hum. Mol. Genet.* **17**, 2238–2243 (2008).
16. Chaves, J. *et al.* Progressive myoclonus epilepsy with nephropathy C1q due to SCARB2/LIMP-2 deficiency: clinical report of two sibs. *Seizure* **20**, 738–40 (2011).
17. Fu, Y.-J. *et al.* Progressive myoclonus epilepsy: extraneuronal brown pigment deposition and system neurodegeneration in the brains of Japanese patients with novel SCARB2 mutations. *Neuropathol. Appl. Neurobiol.* **40**, 551–63 (2014).
18. Gaspar, P. *et al.* Action myoclonus-renal failure syndrome: diagnostic applications of activity-based probes and lipid analysis. *J. Lipid Res.* **55**, 138–145 (2014).
19. Schapira, A. H. V. Glucocerebrosidase and Parkinson disease: Recent advances. *Mol. Cell. Neurosci.* **66**, 37–42 (2015).
20. Siebert, M., Sidransky, E. & Westbroek, W. Glucocerebrosidase is shaking up the synucleinopathies. *Brain* **137**, 1304–1322 (2014).
21. Sidransky, E. *et al.* Multicenter analysis of glucocerebrosidase mutations in Parkinson's disease. *N. Engl. J. Med.* **361**, 1651–61 (2009).
22. Michelakakis, H. *et al.* Evidence of an association between the scavenger receptor class B member 2 gene and Parkinson's disease. *Mov. Disord.* **27**, 400–5 (2012).
23. Hopfner, F. *et al.* The role of SCARB2 as susceptibility factor in Parkinson's disease. *Mov. Disord.* **28**, 538–40 (2013).
24. Maniwang, E., Tayebi, N. & Sidransky, E. Is Parkinson disease associated with lysosomal integral membrane protein type-2?: challenges in interpreting association data. *Mol. Genet. Metab.* **108**, 269–71 (2013).
25. Sardi, S. P., Cheng, S. H. & Shihabuddin, L. S. Gaucher-related synucleinopathies: The examination of sporadic neurodegeneration from a rare (disease) angle. *Prog. Neurobiol.* **125**, 47–62 (2015).
26. Sardi, S. P., Singh, P., Cheng, S. H., Shihabuddin, L. S. & Schlossmacher, M. G. Mutant GBA1 expression and synucleinopathy risk: first insights from cellular and mouse models. *Neurodegener. Dis.* **10**, 195–202 (2012).
27. Sardi, S. P. *et al.* Augmenting CNS glucocerebrosidase activity as a therapeutic strategy for parkinsonism and other Gaucher-related synucleinopathies. *Proc. Natl. Acad. Sci. U. S. A.* **110**, 3537–42 (2013).
28. Rothaug, M. *et al.* LIMP-2 expression is critical for β -glucocerebrosidase activity and α -synuclein clearance. *Proc. Natl. Acad. Sci.* **111**, 15573–15578 (2014).
29. Barton, N. W. *et al.* Replacement therapy for inherited enzyme deficiency--macrophage-targeted glucocerebrosidase for Gaucher's disease. *N. Engl. J. Med.* **324**, 1464–70 (1991).
30. Grabowski, G. A. *et al.* Enzyme therapy in type 1 Gaucher disease: comparative efficacy of mannose-terminated glucocerebrosidase from natural and recombinant sources. *Ann. Intern. Med.* **122**, 33–9 (1995).
31. Zimran, A. & Elstein, D. Management of Gaucher disease: enzyme replacement therapy. *Pediatr. Endocrinol. Rev.* **12 Suppl 1**, 82–7 (2014).
32. Grabowski, G. A., Golembo, M. & Shaaltiel, Y. Taliglucerase alfa: An enzyme replacement therapy using plant cell expression technology. *Mol. Genet. Metab.* **112**, 1–8 (2014).
33. Zimran, A. *et al.* Pivotal trial with plant cell-expressed recombinant glucocerebrosidase, taliglucerase alfa, a novel enzyme replacement therapy for Gaucher disease. *Blood* **118**, 5767–73 (2011).
34. Aerts, J. M. F. G., Hollak, C. E. M., Boot, R. G., Groener, J. E. M. & Maas, M. Substrate reduction therapy of glycosphingolipid storage disorders. *J. Inherit. Metab. Dis.* **29**, 449–456 (2006).
35. Cox, T. *et al.* Novel oral treatment of Gaucher's disease with N-butyldeoxynojirimycin (OGT 918) to decrease substrate biosynthesis. *Lancet* **355**, 1481–1485 (2000).
36. Hughes, D. A. & Pastores, G. M. Eliglustat for Gaucher's disease: trippingly on the tongue. *Lancet* **385**, 2328–2330 (2015).
37. Cox, T. M. *et al.* Eliglustat compared with imiglucerase in patients with Gaucher's disease type 1 stabilised on enzyme replacement therapy: a phase 3, randomised, open-label, non-inferiority trial. *Lancet* **385**, 2355–2362 (2015).
38. Mistry, P. K. *et al.* Effect of Oral Eliglustat on Splenomegaly in Patients With Gaucher Disease Type 1. *JAMA* **313**, 695 (2015).

39. Benito, J. M., García Fernández, J. M. & Ortiz Mellet, C. Pharmacological chaperone therapy for Gaucher disease: a patent review. *Expert Opin. Ther. Pat.* **21**, 885–903 (2011).
40. Boyd, R. E. *et al.* Pharmacological chaperones as therapeutics for lysosomal storage diseases. *J. Med. Chem.* **56**, 2705–25 (2013).
41. Jonsson, L. M. V *et al.* Biosynthesis and maturation of glucocerebrosidase in Gaucher fibroblasts. *Eur. J. Biochem.* **164**, 171–179 (1987).
42. Greenbaum, D., Medzihradzky, K. F., Burlingame, A. & Bogyo, M. Epoxide electrophiles as activity-dependent cysteine protease profiling and discovery tools. *Chem. Biol.* **7**, 569–581 (2000).
43. Greenbaum, D. *et al.* Chemical approaches for functionally probing the proteome. *Mol. Cell. Proteomics* **1**, 60–8 (2002).
44. Hillaert, U. *et al.* Receptor-Mediated Targeting of Cathepsins in Professional Antigen Presenting Cells. *Angew. Chemie Int. Ed.* **48**, 1629–1632 (2009).
45. Blanz, J. *et al.* Disease-causing mutations within the lysosomal integral membrane protein type 2 (LIMP-2) reveal the nature of binding to its ligand β -glucocerebrosidase. *Hum. Mol. Genet.* **19**, 563–572 (2010).
46. Malini, E. *et al.* Role of LIMP-2 in the intracellular trafficking of β -glucosidase in different human cellular models. *FASEB J.* **29**, 3839–52 (2015).
47. Zachos, C., Blanz, J., Saftig, P. & Schwake, M. A Critical Histidine Residue Within LIMP-2 Mediates pH Sensitive Binding to Its Ligand β -Glucocerebrosidase. *Traffic* **13**, 1113–1123 (2012).
48. Zunke, F. *et al.* Characterization of the complex formed by β -glucocerebrosidase and the lysosomal integral membrane protein type-2. *Proc. Natl. Acad. Sci.* **113**, 3791–3796 (2016).
49. Velayati, A. *et al.* A mutation in SCARB2 is a modifier in Gaucher disease. *Hum. Mutat.* **32**, 1232–8 (2011).
50. Witte, M. D. *et al.* Ultrasensitive in situ visualization of active glucocerebrosidase molecules. *Nat. Chem. Biol.* **6**, 907–913 (2010).
51. Kallemeijn, W. W. *et al.* Novel activity-based probes for broad-spectrum profiling of retaining β -exoglucosidases in situ and in vivo. *Angew. Chemie - Int. Ed.* **51**, 12529–12533 (2012).
52. Ran, F. A. *et al.* Genome engineering using the CRISPR-Cas9 system. *Nat. Protoc.* **8**, 2281–308 (2013).
53. Aerts, J. M. *et al.* The occurrence of two immunologically distinguishable beta-glucocerebrosidases in human spleen. *Eur. J. Biochem.* **150**, 565–74 (1985).